A method for *in situ* characterization of tip shape in ac-mode atomic force microscopy using electrostatic interaction

L. Olsson, N. Lin, V. Yakimov, and R. Erlandsson[a)]
Laboratory of Applied Physics, Department of Physics and Measurement Technology, Linköping University, S-581 83 Linköping, Sweden

(Received 27 April 1998; accepted for publication 14 July 1998)

We present a method for *in situ* characterization of the tip shape in atomic force microscopes that can operate in noncontact ac mode. By sweeping the voltage between tip and sample while recording the sample position as it is regulated to give a constant force gradient, we obtain curves giving information about the tip geometry. The measurements were performed in ultrahigh vacuum using electrochemically etched tungsten tips against a surface of doped silicon. Our results show that the sphere model gives a good description of the interaction, and that the radii we obtain are consistent with data from scanning electron microscopy. The method can also be used to estimate the value of the Hamaker constant and the contact potential between tip and sample. © *1998 American Institute of Physics.* [S0021-8979(98)03420-3]

I. INTRODUCTION

The atomic force microscope (AFM)[1] is a powerful tool for topographic surface imaging capable of attaining true atomic resolution. The technique can also be used to measure forces in the sub-nN range[2] and has been adapted for investigations of localized charges,[3] magnetic distributions,[4] and contact potentials.[5] The AFM image is created by moving a sharp tip which is mounted on a flexible cantilever in close proximity to a surface while a feedback system maintains a fixed tip-to-sample separation. When the force microscope is operated in the dc mode, the deflection of the cantilever is kept constant so the tip follows contours of constant force, while in ac-mode operation the change in cantilever resonance properties due to the interaction is used to regulate the separation. In noncontact ac mode operation the tip will never be in repulsive contact with the surface and will, to a first approximation, follow contours of constant force gradient.[6]

The lateral resolution of the AFM is determined by the size of the interaction region, which depends on the sharpness of the tip and the range of the force interaction. In order to properly evaluate the images it is important to have a knowledge of the shape and dimensions of the tip as the recorded data is always a convolution of the sample topography and the tip geometry. Measurements of forces and tribological properties also require that the tip shape is known.[7] Techniques like scanning electron microscopy (SEM) or transmission electron microscopy can be used to characterize the tip outside the AFM, but it would in many cases be advantageous to obtain information about the tip shape without removing it from the instrument. This is particularly the case for force microscopes operating in ultrahigh vacuum, where transferring the tip out of the system can be time consuming and the tips are often subject to *in situ* pretreatments like heating and ion bombardment. A way to characterize the tip is to image a sample with known topography and use deconvolution methods to determine its size and shape.[8] This method requires, however, that calibrated samples are available and that the recorded data goes through a postacquisition deconvolution procedure. The scanning of a calibration sample also involves the risk of damaging the tip. It is thus desirable to have a method that can give a quantitative estimation of the tip geometry which relies on the measurement of a known tip–sample interaction. If conducting tips are used, the electrostatic force is well suited for this purpose as it acts over a long range, is well understood theoretically, and can be controlled by the operator. To obtain a theoretical expression for the electrostatic interaction between a conducting sample and an arbitrary tip shape is complex, but the use of simplified geometries can often give a good approximation for restricted separation ranges. Table I gives the analytical expressions for the force and force gradient corresponding to the plane surface model, the sphere model,[3] and the charged line model.[9] The equipotential surface from a uniformly charged line is a good approximation of a conical tip. The definition of the parameters used in the text are given in the captions to Table I.

A practical method for tip characterization should use a realistic model for the electrostatic interaction and allow the measurements to be interpreted in terms of a geometric parameter like a sphere radius, R, or cone angle, θ, that gives a meaningful description of the tip. Hao, Baró, and Sáenz used the cantilever deflection to measure the force versus tip–sample separation at various bias voltages, and compared the results to different models.[9] To measure the electrostatic interaction by detecting the cantilever deflection is, however, difficult when using the stiffer cantilevers designed for ac-mode operation. It would also be desirable to avoid going into contact with a voltage between tip and sample in order to establish the zero point of the separation, as this can damage the tip.

In this article we present a method to obtain information about the shape and dimensions of the tip using the electro-

[a)]Electronic mail: rag@ifm.liu.se

TABLE I. Analytical expressions for the force and force gradient using different models for the tip shape. The formulas are valid for $d<R$, zero contact potential, and electrically grounded tip. The right-hand column gives the variation in tip–sample separation with sample voltage for fixed force gradient (compare Fig. 2). F: tip force, F': tip force gradient, d: tip-to-sample separation, R: tip radius, θ: tip cone angle, L: tip length, U: sample voltage, H: Hamaker constant.

Model	F	F'	$d\|_{F'=\text{const.}}$
Electrostatic:			
Sphere	$-\dfrac{\pi\epsilon_0 R U^2}{d}$	$\dfrac{\pi\epsilon_0 R U^2}{d^2}$	$\left(\dfrac{\pi\epsilon_0 R}{F'}\right)^{1/2} U$
Charged line (∼cone)	$-\dfrac{\alpha^2}{4\pi\epsilon_0}\ln\left(\dfrac{L}{4d}\right)U^2$	$\dfrac{\alpha^2 U^2}{4\pi\epsilon_0 d}$	$\left(\dfrac{\alpha^2}{4\pi\epsilon_0 F'}\right)U^2$
Plane surface (circular area)	$-\dfrac{\pi\epsilon_0 R^2 U^2}{2d^2}$	$\dfrac{\pi\epsilon_0 R^2 U^2}{d^3}$	$\left(\dfrac{\pi\epsilon_0 R^2}{F'}\right)^{1/3} U^{2/3}$
van der Waals:			
Sphere	$-\dfrac{HR}{6d^2}$	$\dfrac{HR}{3d^3}$	$\cdots$

$\alpha = 2\pi\epsilon_0/Arc\ \sinh[1/\tan(\theta/2)]$.

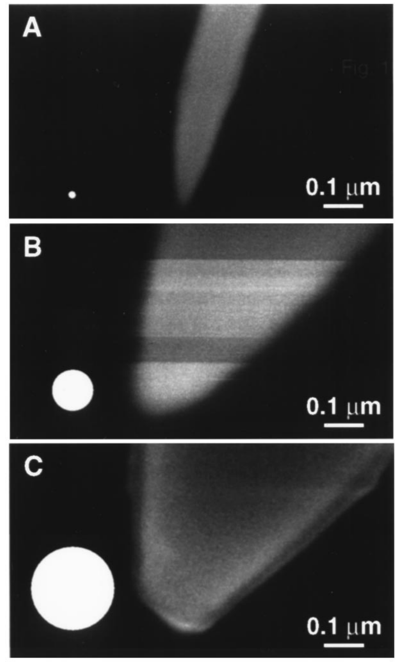

FIG. 1. Scanning electron micrographs of the AFM tip. Tip A: after initial etching, tip B: after first re-etch, and tip C: after second re-etch. The white circular areas show the respective tip radii as determined by the electrostatic method. The intensity variation in the micrograph of tip B is an artefact.

static interaction in an ac-mode force microscope. The method can also be used to estimate the Hamaker constant and measure the contact potential.

II. EXPERIMENT

The measurements were performed in an ultrahigh vacuum AFM system of our own design which uses a fibre-optic interferometer to detect the cantilever motion.[10] The instrument was operated in the ac mode using tungsten tips of three apex shapes (A, B, and C) as shown in the SEM images in Fig. 1. Our cantilever/tip unit was made from a bent and electrochemically etched tungsten wire as described in Ref. 10. This cantilever preparation procedure will routinely give an apex radius which is smaller than the minimum radius of approximately 100 Å that we can resolve in our SEM. The same cantilever was used for all experiments as the tip was re-etched to increase the radius between each measurement series. By using the same cantilever we eliminate the relative error due to the uncertainty in the spring constant determination. A Jeol 220 scanning electron microscope was used to image the tip before and after each re-etching. The cantilever used in the experiments had a length of 1 mm, a diameter of 40 μm, and a resonance frequency of ∼17 kHz. The spring constant was measured to 107 N/m by detecting the deflection when pressing the cantilever against a calibrated spring. This value is consistent with calculations based on the dimensions and resonance frequency of the cantilever.

The sample was cut from an n-doped, polished Si(111) wafer (ρ=5 mΩcm, $N_D = 1\times10^{19}$ As atoms/cm^3)[11] that had been cleaned and heated in the standard way to remove the oxide and obtain the 7×7 reconstruction.[10] This sample provided an atomically flat surface that was kept under ultrahigh vacuum during the entire measurement period. Semiconductor surfaces can under certain conditions give electrostatic forces that are different from metallic systems as the surface charge do not vary in proportion to the bias voltage.[12] A metallic behavior is, however, expected for tip–surface separations larger than the Debye depletion length. For our highly doped material this value is less than 0.5 nm and control measurements using a gold sample confirm the metallic behavior of our silicon surface.

In ac-mode force microscopy, the cantilever is oscillated at or near the resonance frequency. If the variation in force gradient between tip and sample is small over the range that corresponds to the oscillation trajectory of the tip, the force gradient $F' = \partial F/\partial d$ is related to a shift in the cantilever resonance frequency, Δf, by

$$F' = -\frac{2k\Delta f}{f_{\text{res}}}, \tag{1}$$

where k is the cantilever spring constant, d is the tip-to-sample separation, and f_{res} is the resonance frequency of the undisturbed cantilever.[13] The minus sign indicates that the resonance frequency decreases with increasing F' using the normal definition of the interaction potential. In order to characterize the tip geometry we record the z position of the sample normal to the surface, defined relative an arbitrary zero level, as we vary the voltage U applied to the sample while the feedback maintains a constant force gradient. The tip is electrically grounded. For a metallic tip–sample system, these $z(U)$ curves will be symmetric around 0 V, or shifted a small amount due to a contact potential, as the electrostatic force depends on the absolute magnitude of the true potential between tip and surface. For voltages around zero, the interaction is mainly due to the van der Waals force while the electrostatic interaction dominates for $|U|>3$ V for all combinations of R and F' used here. As the curve form depends on how the force gradient varies with tip–sample separation, the $z(U)$ plots will indicate which interaction

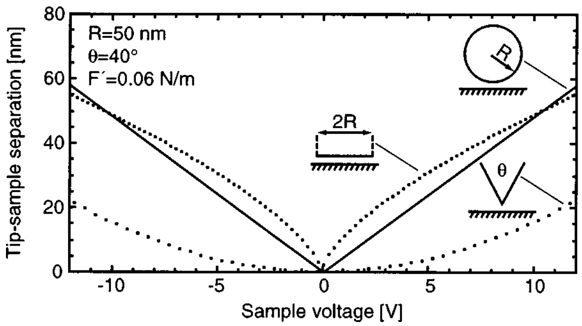

FIG. 2. Theoretical curves showing how the tip-to-sample distance varies with sample voltage if the force gradient is kept constant. The three curves correspond to the electrostatic interaction models presented in Table I. Tip and sample are presumed to be metallic, and the tip is held at ground potential. The parameters are chosen to match the experimental values for tip B used in Fig. 3.

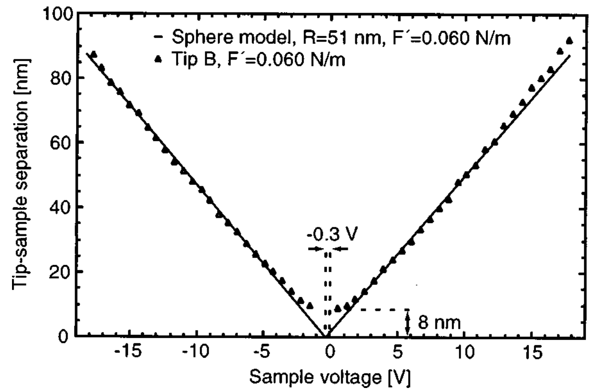

FIG. 3. The curve indicated by triangles show how the tip-to-sample separation d varies with sample voltage U at a constant force gradient of 0.06 N/m, using the B tip. The solid curve represents $d(U+0.3\ \mathrm{V})$ using the analytical expression for the sphere model describing the electrostatic interaction. The 0.3 V offset is due to the contact potential.

model that is applicable. Expressions showing how the separation d varies with sample voltage U at constant force gradient for the different interaction models are given in Table I. It should be observed that the experimental $z(U)$ curves give the sample position related to an arbitrary zero level while the theoretical curves give the tip-to-sample separation d as a function of U. If the electrostatic interaction model is established from the form of the curve it is, however, possible to estimate the absolute separation from the experimental curves by extrapolating the region where the electrostatic interaction dominates to the point were it becomes zero. In this case the experimental curves can be presented as $d(U)$ plots.

To operate the feedback circuit at a fixed force gradient we use the amplitude detection method where the frequency shift of the cantilever is detected by measuring the variation in its oscillation amplitude when it is driven at its undisturbed resonance frequency. In order to control that the oscillation remains harmonic, which is required for Eq. (1) to be valid, we record frequency spectra for different applied voltages and tip-to-sample separations which show that they shift without distortion for the tip–sample separations and oscillation amplitudes used. We also use frequency spectra to fine tune the feedback set point to give the desired frequency shift before we record a $z(U)$ curve. The free oscillation amplitudes varied between 1.2 and 1.5 nm_{p-p}. The force gradient from the bulk of the cantilever has been estimated to be approximately five orders of magnitude smaller than the contribution from the apex region of the tip, and can thus be neglected. All the curves presented have been corrected for unlinearities in the scanner piezomaterial.

III. RESULTS

Figure 2 shows theoretical $d(U)$ curves at constant force gradient calculated using the electrostatic interaction models presented in Table I. As is seen from the figure and the expression in Table I, the $d(U)$ curve for the sphere model has a linear slope that depends on R which implies that it is possible to determine the tip radius from an experimental $z(U)$ curve by measuring its slope in the region where the electrostatic force dominates.

Figure 3 shows an experimental curve for tip B recorded at a constant force gradient of 0.060 N/m, corresponding to a frequency shift of 5 Hz. The solid line is a theoretical curve using the sphere model for the electrostatic interaction with $R=51$ nm where a 0.3 V offset has been added to U in order to account for the shift due to the contact potential. The zero point for the separation is defined from the point where the extrapolations of the linear parts of the experimental curve intersect, which allows us to present the data as a $d(U)$ plot. The nearly linear behavior of the experimental data for $|U| > 3$ V indicates that the sphere model is a good approximation. Even though the approximate formulas for the sphere model given in Table I require that $d<R$, the $d(U)$ curve in Fig. 3 is close to linear for tip–sample separations larger than the estimated tip radius. Differentiation of the full expression (not shown) for the electrostatic force which is valid for all values of R shows, however, that the relative error for large R is smaller for the force gradient than for the force, which could explain this observation.

In order to further check the validity of the sphere model, we have recorded $d(U)$ curves at different force gradients for each tip. Figure 4(a) shows $d(U)$ curves for tip B where we have used a straight line fit for the data points corresponding to the voltage range $4\ \mathrm{V} < |U| < 12$ V to calculate the tip radius. The same measurement has been performed for tips A and C (not shown) and for each tip we obtain R values that agree to within 5%.

Figure 4(b) shows $d(U)$ curves for the tips A, B, and C. Approximating straight lines to the data points in the voltage range $4\ \mathrm{V} < |U| < 12$ V we obtain the values $R_A = 9$ nm, $R_B = 51$ nm, and $R_C = 104$ nm, which are also indicated as filled circles on the SEM micrographs in Fig. 1.

IV. DISCUSSION

Belaidi, Girard, and Leveque[14] calculated the electrostatic tip force with a model using a sum of equivalent charges whose equipotential surface was fitted to the geometry of a cone ending in a sphere with radius R, and made comparisons with calculations using simplified models. They concluded that the sphere model worked well for $d<R$,

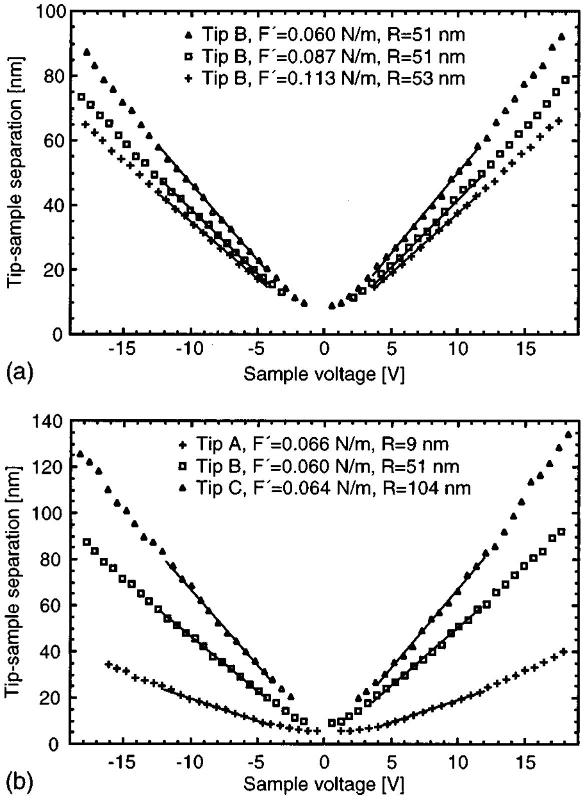

FIG. 4. (a) The graphs shows how the tip-to-sample separation d varies with sample voltage for three different values of the force gradient using tip B. Linear curve fits were done between $|U|=4$ V and $|U|=12$ V to estimate the tip radius. (b) The graphs shows how the tip-to-sample separation d varies with sample voltage for tips A, B, and C. Linear curve fits were done between $|U|=4$ V and $|U|=12$ V to estimate the tip radius for each tip. The R values are taken as the mean value of the slope calculated from the positive and negative half of the curves. The measured R values given are those shown as filled circular regions in Fig. 1.

while the charged-line model was a better choice in an intermediate range where $R<d<L$, L being the length of the tip. They also noted that the force on the tip apex is best described by the sphere model, while the force acting on the sides is given by the charged-line model. Experimental data using a tungsten tip presented by Hao, Baró, and Sáenz[9] also showed that the sphere model worked well for small separations while larger separations required that the elongated part of the tip was taken into account. The nearly linear slope of our $d(U)$ curves confirm the validity of the sphere model. Comparing the curves in Fig. 4(b) with the actual shape of the tips shown in the micrographs in Fig. 1, it is seen that tip *B*, which has the most rounded apex, also gives the best approximation to a straight line. Tip *C* has a more truncated apex shape and the radius of tip *A* is too small to be well characterized by the SEM. Very sharp silicon tips that give atomic resolution in ac-mode AFM are expected to have faceted rather than spherical apex shapes as has been deduced from frequency versus distance data.[15] Even though real tips cannot be expected to have a perfectly spherical apex, the overall agreement seen in Fig. 1 shows that the method gives a good indication of tip sharpness.

Measurements using tip *C* against an evaporated Au film with a root mean square roughness of 1.5 nm gave the same values for the tip radius as when using the Si(111) surface.

An interesting aspect of the $d(U)$ curves is that they simultaneously provide information about the shape of the tip (the form of the curve), its absolute size (the slopes of the curve if the tip is spherical) and the tip-to-sample separation at the closest point (the separation between the minimum and the intersection of the extrapolated linear parts of the curve). As the curves are recorded at a constant force gradient, the information needed to calculate the strength of the van der Waals interaction using the formula in Table I is in principle available, provided that the sphere model can be applied. With values from Fig. 3 we obtain a Hamaker constant of 1.8×10^{-18} J. This value is higher than those quoted for metallic systems ($3-5\times10^{-19}$ J)[16] but it should be kept in mind that there are several factors that can affect the accuracy of this estimation. It is not obvious that the tip radius calculated for the longer range electrostatic interaction can be used for the calculation of the Hamaker constant which can be expected to depend on the details of the tip apex on a smaller scale. Preliminary data indicate that tips that have been heated *in situ* in order to remove the oxide and the carbon contamination deposited in the SEM will give lower Hamaker constants consistent with metallic systems. This could be an effect of tip cleaning but it is also possible that tip heating smoothens the tip apex, making the radius calculated from the electrostatic measurement applicable also for the estimation of the van der Waals force.

The shift due to the contact potential seen in Fig. 3 indicates a 0.3 eV higher work function for the tip compared to the silicon sample. As contact potential measurements are extremely sensitive to the state of the surfaces[5] and our tips are likely to have an oxide layer and a carbon contamination from the SEM measurements, we have not attempted a rigorous interpretation in terms of work functions. It is, however, clear that the method has the potential to be used for work function determinations with high lateral resolution.

V. CONCLUSIONS

We have presented a method for tip characterization in ac-mode AFM based on measuring the sample position as a function of bias voltage while the feedback circuit maintains a constant force gradient. Our electrochemically etched tungsten tips are well described by the sphere model for the separations we have investigated. Results from tips with different radii are compared with SEM micrographs, showing that a quantitative estimation of the tip geometry can be obtained. The tip characterization is done while the feedback is operating, and does not require any additional measurements to determine the absolute value of the tip–sample separation, thus minimizing the risk for tip damage. The method is well suited for routine checks of tip quality as it does not need any modifications of the normal instrument configuration. The data we record contains all information necessary to calculate the Hamaker constant and contact potential of the tip–sample system, but more work is needed to develop these aspects of the method.

ACKNOWLEDGMENTS

The AFM activity at Linköping University is supported by the Swedish Research Council for Engineering Sciences (T.F.R.).

[1] G. Binnig, C. F. Quate, and Ch. Gerber, Phys. Rev. Lett. **56**, 930 (1986).
[2] W. A. Ducker, T. J. Senden, and R. M. Pashley, Nature (London) **353**, 239 (1991).
[3] B. D. Terris, J. E. Stern, D. Rugar, and H. J. Mamin, Phys. Rev. Lett. **63**, 2669 (1989).
[4] D. Rugar, H. J. Mamin, P. Guethner, S. E. Lambert, J. E. Stern, I. McFadyen, and T. Yogi, J. Appl. Phys. **68**, 1169 (1990).
[5] M. Nonnenmacher, M. P. O'Boyle, and H. K. Wickramasinghe, Appl. Phys. Lett. **58**, 2921 (1991).
[6] Y. Martin, C. C. Williams, and H. K. Wickramasinghe, J. Appl. Phys. **61**, 4723 (1987).
[7] R. W. Carpick, N. Agrait, D. F. Ogletree, and M. Salmeron, J. Vac. Sci. Technol. B **14**, 1289 (1996).
[8] J. S. Villarrubia, Surf. Sci. **321**, 287 (1994).
[9] H. W. Hao, A. M. Baró, and J. J. Sáenz, J. Vac. Sci. Technol. B **9**, 1323 (1991).
[10] L. Olsson, R. Wigren, and R. Erlandsson, Rev. Sci. Instrum. **67**, 2289 (1996).
[11] Virginia Semiconductor Inc., Fredericksburg, VA, USA.
[12] S. Hudlet, M. Saint Jean, B. Roulet, J. Berger, and C. Guthmann, J. Appl. Phys. **77**, 3308 (1995).
[13] R. Erlandsson, G. M. McClelland, C. M. Mate, and S. Chiang, J. Vac. Sci. Technol. A **6**, 266 (1988).
[14] S. Belaidi, P. Girard, and G. Leveque, J. Appl. Phys. **81**, 1023 (1997).
[15] F. J. Giessibl, Phys. Rev. B **56**, 16 010 (1997).
[16] J. N. Israelachvili, *Intermolecular and Surface Forces*, 2nd ed. (Academic, London, 1985), p. 187.